Modeling the Process-Zone Kinetics of Polycarbonate

A. KIM,[1,*] L. V. GARRETT,[2] C. P. BOSNYAK,[3] and A. CHUDNOVSKY[1]

[1]Department of Civil Engineering, Mechanics and Metallurgy (M/C 246), University of Illinois at Chicago, P.O. Box 4348, Chicago, Illinois 60680; [2]Wright Laboratory, Aircrew Enclosure Group (WL/FIVR) Wright-Patterson AFB, Ohio 45433-6553; [3]The Dow Chemical Company, Polycarbonate R&D, B-1470A, 2301 N. Brazosport Blvd., Freeport, Texas 77541

SYNOPSIS

A thermodynamic model for the equilibrial process zone ahead of a crack in polycarbonate is developed from the recently proposed Chudnovsky model and experimental characterization of the process zone. Based on the model, the force for evolution of the process zone is proposed from the consideration of irreversible thermodynamics and chemical reaction theories. The experimental data reported in our previous paper are well described by the equilibrial process zone model and a new kinetic equation. © 1993 John Wiley & Sons, Inc.

1. INTRODUCTION

In a previous paper, we reported the evolution of the process zone ahead of a crack under stress-relaxation at a constant crack length in a polycarbonate.[1] The evolution of the process zone was evaluated in terms of the relative deviation of the current process zone size from its equilibrial value. However, this parameter did not allow us to generate a master curve for the various experimental conditions. The goal of this paper is to construct a constitutive equation for process zone growth employing thermodynamic considerations.

A thermodynamic model for an equilibrial process zone in polymers was recently proposed by Chudnovsky[2] and its validity was supported by the experimental studies on various polyethylenes.[3,4] The essence of the Chudnovsky model (CM) is that the process zone can be considered as a homogenous second phase, i.e., transformed material, and thus the shape and the size of the process zone are derived from the phase equilibrium conditions.

The experimental examination of the CM has been performed on polyethylene for which the assumption of the homogeneity of the transformed (drawn) material within the process zone is quite adequate. However, the observation of the process zone in polycarbonate (PC) shows an important difference: It consists of shear bands whose density varies noticeably within the zone. Similarly, in examination of the neck formation under uniaxial tension of PC, one observes a spectrum of intermediate stages between the initial and fully drawn (transformed) material. In the present paper, we improve the CM to account for the variable extent of transformation of material within the process zone. Further, we employ the improved model to determine the process zone driving force and then formulate an appropriate kinetic equation following the framework of irreversible thermodynamics. An analysis of the parameters of the model as well as a comparison with experimental data are also presented.

2. REVIEW OF THE CM MODEL

Let G be the Gibbs potential of the system described in Figure 1, and V_{pz}, the domain occupied by the process zone. Then, for the isothermal condition, the equilibrial domain V_{pz} of the process zone corresponds to the minimum of G, i.e.:

$$\left.\frac{\delta G(\sigma_\infty, V_{pz})}{\delta V_{pz}}\right|_{l=\text{const}} = 0 \qquad (1)$$

Here, G is a functional of the domain V_{pz} and a function of crack length l and applied remote stress σ_∞.

* To whom correspondence should be addressed.

Journal of Applied Polymer Science, Vol. 49, 877–883 (1993)
 CCC 0021-8995/93/050877-07

Following Ref. 2, we employ the Eshelby method to evaluate a variation of the Gibbs potential due to a virtual migration of the process zone boundary:

$$\delta G = -\int_{\partial V_{pz}} \delta\xi_i (P_{ij}^0 - P_{ij}^{pz}) n_j \, d\Gamma \qquad (2)$$

For evaluation of the Gibbs potential, G, of a crack with the surrounding process zone consisting of the second phase [see Fig. 2(a)], the two-phase system was decomposed into its elements as shown in Figure 2(b). The first element results from removal of the process zone and substituting its action with an equivalent traction σ_{dr} along the interface (σ_{dr} is the drawing stress). The second element is the process zone V_{pz} within which the original material submitted to σ_{dr} undergoes the transformation (drawing). The width, w_0, of the layer of the original material in Figure 1 that underwent transformation varies along the process zone length x_1 and is initially unknown. The resulting width, $w^*(x_1)$, of the process zone is $w^*(x_1) = \lambda(x_1) w_0(x_1)$, with λ being the draw ratio and assumed constant within the process zone. The displacement caused by the transformation at the interface shown in element 2 of Figure 2(b) is $w^*(x_1) - w_0(x_1)$.

For coherency of the interface, it is required that the opening of a slit in element 1 be equal to the displacement of the boundary of element 2. For a slender process zone, the displacement of element 1 can be approximated as the crack-opening displacement, Δ, thus leading to the following compatibility equation:

$$\Delta(x_1, l, l_a) = w^* - w_0 \qquad (3)$$

Then, the width $w_0(x_1)$ of the initial strip that is transformed into the process zone is directly related to the crack-opening displacement of element 1 in Figure 2(b):

$$w_0(x_1) = \Delta(x_1, l, l_a)(\lambda - 1)^{-1} \qquad (4)$$

Thus, the volume V_{pz} of the initial material can be expressed as

$$V_{pz} = z_0 \int_l^{l+l_a} \Delta(x_1, l, l_a)(\lambda - 1)^{-1} \, dx_1 \qquad (5)$$

where z_0 is the initial thickness of the specimen. The process-zone shape is thus uniquely determined by the process zone length, l_a, because the crack-opening displacement depends on l, σ_∞, σ_{dr}, and l_a. The condition for the minimum Gibbs potential for two-phase system equilibrium can be written as

$$\left.\frac{dG(\sigma_\infty, l, l_a, \sigma_{dr}, \lambda)}{dl_a}\right|_{l=\text{const}} = 0 \qquad (6a)$$

$$\left.\frac{d^2G}{dl_a^2}\right|_{l=\text{const}} > 0 \qquad (6b)$$

Equation (6a) leads to the following equation[2]:

$$K^{tot}(K^{tot} + \tilde{\gamma} K(\sigma_{dr})) = 0 \qquad (6c)$$

and the inequality eq. (6b) ensures the uniqueness of the solution, i.e.:

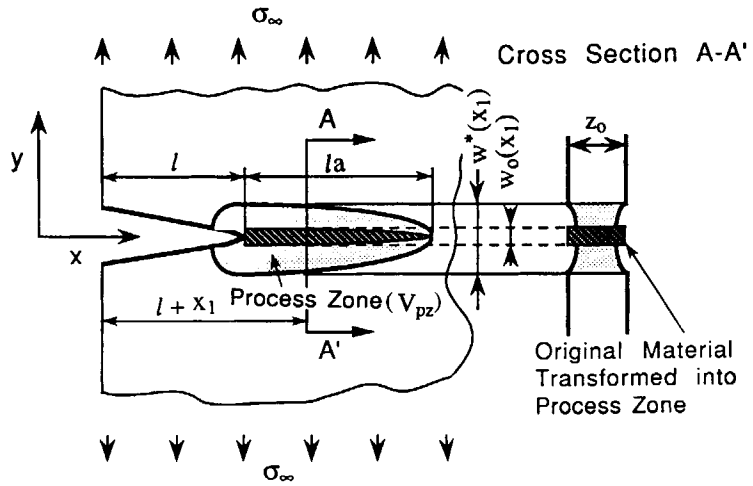

Figure 1 Schematic diagram of a crack and process zone in PC.

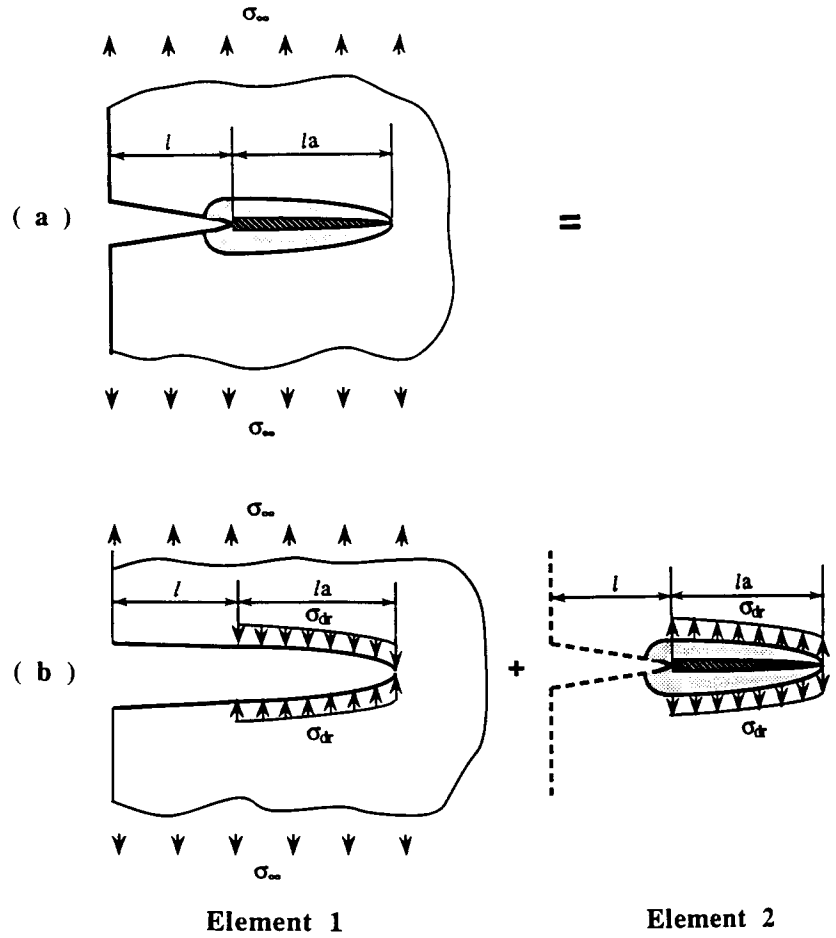

Figure 2 A model for the computation of the Gibbs potential: Element one is obtained from removal of the process zone and substituting its action with an equivalent traction σ_{dr} along the interface, and element two is obtained from the process zone V_{pz} within which the original material submitted to σ_{dr} undergoes the transformation.

$$K^{tot} + \tilde{\gamma} K(\sigma_{dr}) = 0 \qquad (7)$$

Here, K^{tot} is the stress intensity factor (SIF) for element 1 of Figure 2(b), and $K(\sigma_{dr})$, the SIF for the same element with the absence of σ_{∞}. $\tilde{\gamma}$ represents $2\gamma^*/((\lambda - 1)\sigma_{dr})$, where γ^* is the specific transformation energy. This solution leads to the equilibrial process-zone size and shape, which agree well with experimental observations on polyethylene and thin film PC.[2,3,10]

3. IMPROVEMENT OF THE MODEL

As mentioned previously, PC was observed to undergo nonhomogeneous transformation within the process zone. Figure 3 shows the optical micrograph in polarized light and the schematic diagram of the two intersecting families of shear bands in cross section A–A′. We consider the individual shear band as transformed material. Between the shear bands, the material appears to be untransformed. During the evolution of the process zone, drawing progresses by (a) an increase of the number of shear bands and (b) an increase of the width of the individual shear bands at the expense of the neighboring untransformed material.[5] The various stages of the drawn state correspond to different densities of the shear bands.

To characterize an intermediate transformation, we introduce an extent of transformation ζ. $\zeta = 0$ corresponds to the original state and $\zeta = 1$ is associated with the fully transformed state. The thinning of the cross section is a cumulative effect of the shear banding, as illustrated in Figure 3. The thinning and the draw ratio, λ, are uniquely related since the den-

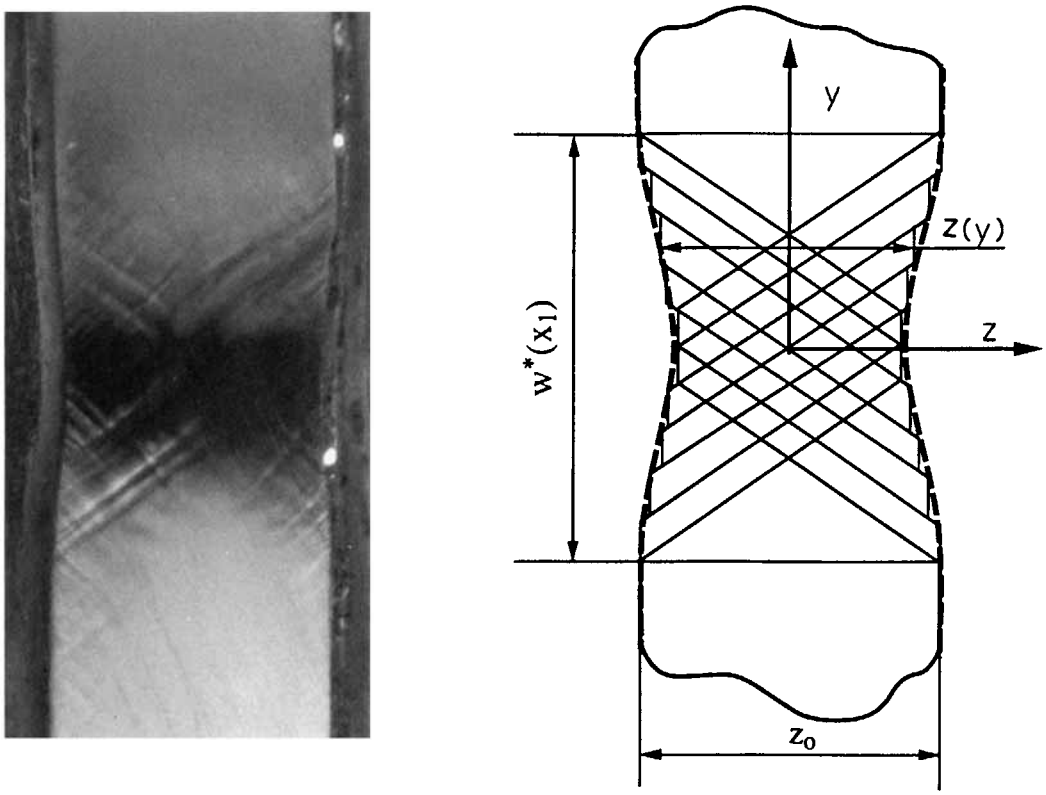

Figure 3 Micrograph and schematic diagram of intersecting families of shear bands in a cross section of the process zone.

sity of transformed material is practically unchanged (a few percent).[3] The extent of transformation ζ is simply related to the draw ratio λ:

$$\zeta = \left(\frac{\lambda - 1}{\lambda}\right)\left(\frac{\lambda^*}{\lambda^* - 1}\right) \tag{8}$$

where λ^* is the draw ratio for fully transformed material and λ is a variable draw ratio reflecting a current extent of transformation. A correspondence between the extent of shear banding and λ has been discussed in our previous paper.[1] It has also been found that the extent of transformation varies within the analyzed process zone. Moreover, the distributions of ζ differ for a process zone formed under different conditions.

Let us consider an average draw ratio $\lambda(x_1)$ for the cross section at x_1:

$$\lambda(x_1) = \frac{1}{w^*}\int_{-w^*/2}^{w^*/2} \frac{z_0}{z(x_1, y)}\, dy \tag{9}$$

Here, z_0 represents the thickness of original material, and z, that in the process zone. Then, the average extent of transformation ζ in the cross section with coordinate "x_1" (see Fig. 1) is given as

$$\zeta(x_1) = \left[\frac{\lambda(x_1) - 1}{\lambda(x_1)}\right]\left(\frac{\lambda^*}{\lambda^* - 1}\right) \tag{10}$$

The thinning profiles presented in Figure 11 of Ref. 1 were used to give the average extent of transformation, $\zeta(x_1)$, and the average draw ratio, $\lambda(x_1)$, along the process zone. Shown in Figure 4 are the values of $\zeta_{eq}(x_1)$ as a function of x_1 normalized by the equilibrial process zone size, $l_{a(eq)}$, for the various fixed displacements. Notice in Figure 4 the similarity of the shape of $\zeta[x_1/l_{a(eq)}]$ and the monotonic increase of the amplitude of $\zeta_{eq}(x_1)$ with the displacement. This suggests that the evolution of the extent of transformation follows a self-similar pattern, which can be formally expressed as follows:

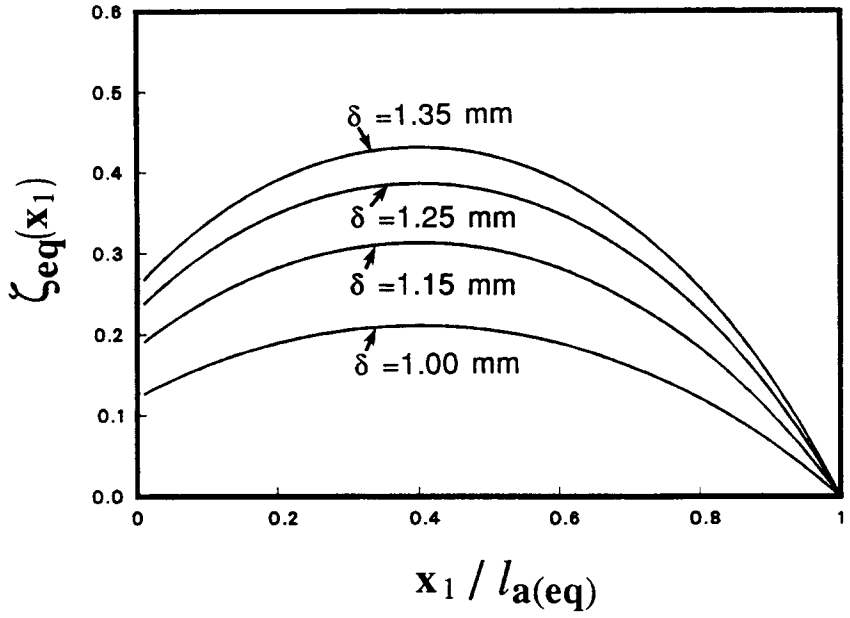

Figure 4 Profiles of average extent of transformation as function of $x_1/l_{a(eq)}$ for various applied displacements.

$$\zeta\left[\frac{x_1}{l_a(t)}, t\right] = \frac{l_a(t)}{l_{a(eq)}}\,\zeta_{eq}\left(\frac{x_1}{l_a}\right) \tag{11}$$

Here, t is time. To evaluate the Gibbs potential, we first need to introduce an effective specific energy, γ, which is related to ζ as follows:

$$\gamma\left[\frac{x_1}{l_a(t)}, t\right] = \gamma^*\zeta\left[\frac{x_1}{l_a(t)}, t\right] \tag{12a}$$

γ^*, in thermodynamic terms, is the difference in chemical potential (per unit volume) across the boundary of untransformed and fully transformed material. Then, the dimensionless factor $\tilde{\gamma}$ also becomes a function of x_1 and time:

$$\tilde{\gamma}\left[\frac{x_1}{l_a(t)}, t\right] = \frac{2\gamma\left[\frac{x_1}{l_a(t)}, t\right]}{\left[\lambda\left(\frac{x_1}{l_a}\right) - 1\right]\sigma_{dr}} \tag{12b}$$

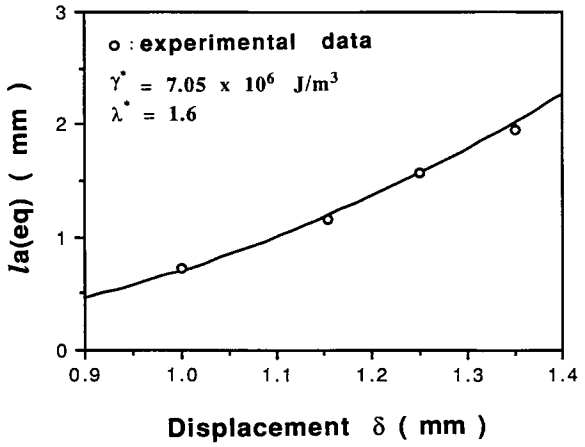

Figure 5 Equilibrial process zone size as a function of applied displacements. The solid line represents the theoretical solution.

At equilibrium, the Gibbs potential depends explicitly on $l_{a(eq)}$, similar to that in the CM, as well as implicitly through the extent of transformation. As a result, eq. 6(a), which is the necessary condition of the minimum Gibbs potential, is rewritten as

$$\left.\frac{\partial G}{\partial l_a}\right|_{l=\text{const}} + \frac{\delta G}{\delta \zeta}\frac{d\zeta\left(\frac{x_1}{l_a}\right)}{dl_a} = 0 \tag{12c}$$

Equation (12c) determines the size of the equilibrial process zone. Figure 5 shows the solution of eq. (12c) (solid line) with $\gamma^* = 7.05 \times 10^6\,\text{J/m}^3$ for the various fixed displacement conditions. The experimental data points are shown by the open circles. Only one parameter is employed in the above treatment for the four experimental conditions reported.

The justification of this value comes from independent tests using the neck formation in simple tension combined with calorimetric determination of the residual strain energy stored in the trans-

formed (necked) material and estimation of heat generation during the transformation.

4. DRIVING FORCE FOR EVOLUTION OF THE PROCESS ZONE

The force on an interface between the original material and the process zone can be defined following Eshelby.[6] In our case, the evolution of the interface is uniquely determined by the process-zone length, l_a, as a function of time. The driving force X_{pz} is determined as

$$X_{pz} = -\left.\frac{dG}{dl_a}\right|_{l=\text{const}} \tag{13}$$

Repeating the arguments prior to eq. (12c) on the dependency of G on l_a, the process-zone driving force can be presented as

$$X_{pz} = -\left[\left.\frac{\partial G}{\partial l_a}\right|_{l=\text{const}} + \frac{\delta G}{\partial \zeta}\frac{d\zeta\left(\frac{x_1}{l_a}\right)}{dl_a}\right] \tag{14}$$

The details of the calculation of eq. (14) will be reported separately. If the transformation of material within the process zone is homogeneous, the CM is recovered. It corresponds to the first term in the rhs of the eq. 14. Figure 6 shows the dependency of the process-zone driving force as a function of $l_a/l_{a(eq)}$ for the four experimental displacement conditions. At equilibrium, the process-zone driving force is zero.

5. THE KINETIC EQUATION OF PROCESS ZONE EVOLUTION

In irreversible thermodynamics for systems close to equilibrium, the rate of change toward the equilibrium is assumed to be proportional to the corresponding driving force, X. In our case, the rate of approaching equilibrium is defined by the rate of changes in l_a, i.e., $\dot{l}_a$. Thus, a kinetic equation can be written as

$$\dot{l}_a = kX_{pz} \tag{15}$$

A different approach has been widely considered in studies of failure kinetics. For example, Zhurkov in his studies of the kinetics of fracture of solids under creep conditions found that a wide range of materials followed a stress-biased Ree–Eyring failure kinetic equation[7]:

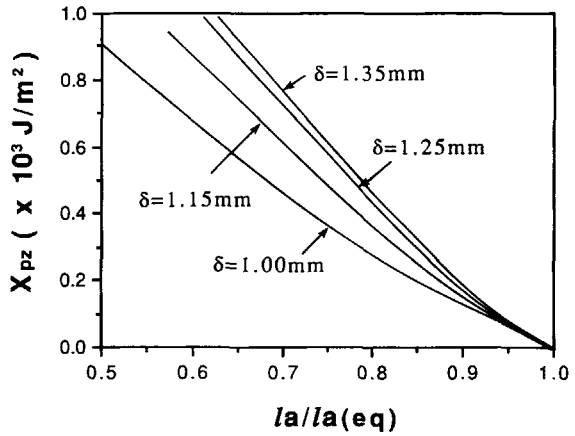

Figure 6 Process zone driving force as function of $l_a/l_{a(eq)}$ for various applied displacements.

$$t_f = A_0 \exp\left(\frac{U - \phi\sigma}{RT}\right) \tag{16}$$

where t_f is the time to failure; T, the absolute temperature; R, the gas constant; A_0, the characteristic time; and ϕ, a factor accounting for the effectiveness of reducing the activation energy, U, by the applied stress, σ. Equation (16) was applied to uniaxial specimens of small diameter for which the fracture propagation time was negligible compared to the crack initiation time.

An energy release rate-biased Ree–Eyring equation was proposed with the argument that the crack rate $\dot{l}$ is inversely proportional to the fracture time on the molecular level and the stress at the crack tip is proportional to the energy release rate G_1 by a relationship such as $\sigma = G_1/\Delta$, where Δ is the crack-opening displacement:

$$\dot{l} = A_1 \exp\left[-\frac{(U - \alpha G_1)}{RT}\right] \tag{17}$$

where $\dot{l}$ is crack velocity and A_1 and α are constants. Equation (17) was adapted in studies of crack growth in PMMA.[8] A similar kinetic equation for alcohol-assisted craze growth in PC was proposed.[9] The shortcoming of these types of exponential equations is the absence of an equilibrial state.

The driving force, X_{pz}, can be decomposed into two parts, namely, a resistive and a driving part:

$$X_{pz} = -\frac{dG}{dl_a} = -\left[\gamma^* \frac{\partial V_{tr}}{\partial l_a} - \left(-\frac{\partial \Pi}{\partial l_a}\right)\right] \tag{18}$$

where V_{tr} is the transformed volume of the process zone and Π is the potential energy of the system.

The resistive part has an analogy with the activation energy, U, and the driving part with the energy release rate, G_1, in eq. (17).

The Arrhenius equation was first developed to account for the temperature dependency of the reaction rate constant, k, in chemical kinetics. Equation (15) resembles that of a first-order chemical reaction, and, therefore, adapting the Arrhenius assumption of k with incorporation of an activation energy reduced by the process zone driving force, we propose the following equation for the kinetic coefficient in eq. (15):

$$k = k_0 \exp\left(-\frac{U - \alpha X_{pz}}{RT}\right) \qquad (19)$$

where α is a constant with units m^2/mol. Finally, combining eq. (19) with (15), we arrive at a new kinetic equation as follows:

$$\dot{l}_a = \left[k_0 \exp\left(-\frac{U - \alpha X_{pz}}{RT}\right)\right] X_{pz} \qquad (20)$$

Note that eq. (20) accounts for an equilibrial state ($\dot{l}_a = 0$ when $X_{pz} = 0$) and becomes increasingly nonlinear with increasing X_{pz}, i.e., with increasing departure from the equilibrium.

Since the experiments reported in Ref. 1 were performed at one temperature, eq. (20) is simplified and the data cast as $\ln(\dot{l}_a)$ vs. X_{pz}, shown in Figure 7. The solid line indicates the fit of eq. (20) with a constant α as 16.39×10^3 (m^2/kmol). The unit of k_0 is $m^4/(J\,s)$. The strongly nonlinear kinetics data are now collapsed into a master curve.

6. CONCLUSION

An improvement to the Chudnovsky model is made that accounts for nonhomogeneous transformation of material within a process zone surrounding a crack.

The distribution of the extent of transformation was experimentally determined in these studies. Further improvement of the model using the variation of the Gibbs potential should allow for prediction of the distribution without experimental determination.

The driving force for the process-zone evolution is evaluated and a new kinetic equation incorporating the driving force is proposed that leads to a master curve for the observed growth of the process zone of polycarbonate under various loading histories.

The fundamental significance of the constants k_0 and α in eq. (20) and their relation to intrinsic material parameters as well as the applicability of the equation to account for temperature and various loading conditions are subjects for future scrutiny.

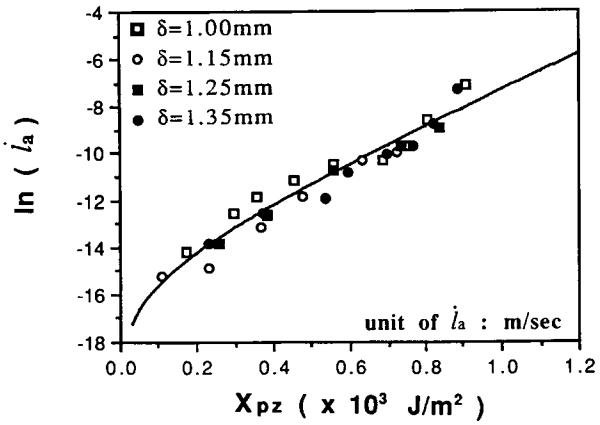

Figure 7 A master curve for the PC process zone kinetics.

The financial support from Wright Laboratory provided through the Air Force Office of Scientific Research (Contract No. AFOSR-89-0105) and the Dow Chemical Co. are gratefully acknowledged for their many useful discussions.

REFERENCES

1. A. Kim, L. V. Garrett, C. P. Bosnyak, and A. Chudnovsky, *J. Appl. Polym. Sci.*, to appear.
2. A. Stojimirovic and A. Chudnovsky, to appear.
3. K. Kadota and A. Chudnovsky, in *Proceedings of the ASME Winter Annual Meeting*, 1991, Vol. MD29, p. 101.
4. A. Stojimirovic, K. Kadota, and A. Chudnovsky, *J. Appl. Polym. Sci.*, **46**, 1051 (1992).
5. M. Ma, K. Vijayan, A. Hiltner, and E. Baer, *J. Mater. Sci.*, **24**, 2687 (1989).
6. J. D. Eshelby, *Inelastic Behavior of Solids*, McGraw-Hill, New York, 1970, pp. 115.
7. S. N. Zhurkov, *Int. J. Fracture*, **1**, 311 (1965).
8. A. G. Atkins, C. S. Lee, and R. M. Caddell, *J. Mater. Sci.*, **10**, 1381 (1975).
9. M. A. Kirloskar and J. A. Donovan, *Polym. Eng. Sci.*, **27**, 124 (1987).
10. A. M. Donald and E. J. Kramer, *J. Mater. Sci.*, **16**, 2977 (1981).
11. K. Schonert, H. Umhauer, and W. Klemm, in *Proceedings of the Second International Conference on Fracture*, Brighton, England, 1969, p. 474.
12. J. A. Kies and A. B. J. Clark, in *Proceedings of the Second International Conference on Fracture*, Brighton, England, 1969, p. 483.

Received July 21, 1992
Accepted November 17, 1992